Carpathian Journal of Earth and Environmental Sciences, July 2017, Vol. 12, No. 2, p. 571 - 582

CROP EVAPOTRANSPIRATION VARIATION UNDER CLIMATE CHANGE IN SOUTH EAST EUROPE DURING 1991-2050

Mărgărit-Mircea NISTOR[1*], Francesco RONCHETTI[2], Alessandro CORSINI[2], Sorin CHEVAL[3], Alexandru DUMITRESCU[4], Praveen KUMAR RAI[5], Dănuţ PETREA[6] & Ştefan DEZSI[6]

[1]Nanyang Technological University, School of Civil and Environmental Engineering, 42 Nanyang Avenue, Singapore, e-mail: margarit@ntu.edu.sg, renddel@yahoo.com

[2]University of Modena and Reggio Emilia, Department of Chemical and Geological Sciences, 103 Via Campi, Modena, 41125, Italy, e-mail: francesco.ronchetti@unimore.it, alessandro.corsini@unimore.it

[3]University of Bucharest, ICUB, 36-46 M. Kogălniceanu Blvd, Bucharest, 050107, Romania, e-mail: sorincheval@yahoo.com

[4]National Meteorological Administration, 97 Şos. Bucureşti-Ploieşti, Bucharest, 013686, Romania, e-mail: alexandru.dumitrescu@gmail.com

[5] Banaras Hindu University, Department of Geography, Institute of Science, Varanasi-221005, U.P. India, e-mail: rai.vns82@gmail.com

[6]University of Babeş-Bolyai, Faculty of Geography, 5-7 Clinicilor Street, Cluj-Napoca, Romania, e-mail:, e-mail: danut.petrea@ubbcluj.ro, stefan.dezsi@ubbcluj.ro

Abstract: The crop evapotranspiration computing is a complex matter from many points of view, but also it represents a useful parameter in hydrological and climate studies. Due to climate changes, the natural systems are coming to be negatively affected. The seasonal and annual crop evapotranspiration under current climate (1991-2020) and future climate (2021-2050) were analysed using the mean annual temperature, mean annual precipitation, and mean monthly potential evapotranspiration for average of 30 years. The spatial distribution of crop evapotranspiration was calculated considering the evapotranspiration coefficients taken from literature using four stages of crops growth. Additionally, the absolute and relative changes of the annual crop evapotranspiration were carried out. The annual crop evapotranspiration varies in the actual period from 56 mm to 1297 mm, while in the future period the annual crop evapotranspiration varies from 59 mm to 1410 mm, which implies the impact of future climate warming on the crop evapotranspiration in the South East Europe. The heights values were identified in the South of Greece, in the southwestern sides of Romania, in the East sides of Bulgaria, Croatia and European Turkey. The maximum seasonal crop evapotranspiration were found in the mid-season, both for present and future. The minimum values of seasonal crop evapotranspiration were obtained in the cold season, when the mean air temperature and crop coefficients are lower. The absolute and relative changes indicate the high values in the South and southwestern sides of the South East Europe.

Keywords: climate change, crop evapotranspiration, land cover, crop coefficient, South East Europe.

1. INTRODUCTION

Global warming is an important issue in the last decades, both from quotidian point of view, but much more from scientifically interest as part of researches for our planet. In both cases, the accent is coming to debate the affected systems, but also the resources which can be drastic in danger due to climate change impact. The most sensitive systems at climate change are the glaciers and its retreating is a consequence of climate warming in many places of the Globe (Haeberli et al., 1999; Kargel et al., 2005; Oerlemans, 2005; Shahgedanova et al., 2005; Dong et al., 2013; Xie et al., 2013; Elfarrak et al., 2014; Nistor & Petcu, 2015; Păcurar, 2015). Changes in fresh water resources have already been observed into rivers flow reductions, melting of icecaps, reduced recharge of aquifers in karst areas and decreasing of groundwater levels (Collins, 2008; Aguilera & Murillo, 2009; Hidalgo et al., 2009; Piao et al., 2010;

Jiménez Cisneros et al., 2014). Parmesan & Yohe (2003), Kløve et al., (2014) called the negative impact of climate change on groundwater. Yustres et al., (2013) announced the decrease of water table and reduced flow discharge of springs in many regions of the Globe due to climate change.

South East Europe represents a large and diversified region of Europe, where the agriculture and water resources are close depended by climate conditions. Any few climate variations may conducts at undesirable consequences in many sides of the region, regarding long periods with drought, desertification, and increase in groundwater vulnerability and biodiversity modifications (Prăvălie, 2014; Prăvălie et al., 2014). Considered the third most important parameter in climatology, the evapotranspiration plays an essential role also in the hydrology and hydrogeology studies, but also the evapotranspiration indicates the exchanges between plants and atmospheric systems (Chen et al., 2006). This is coming because of evapotranspiration data required for calculations of effective precipitations, water balance, and also for the new technology of water modelling.

Temperature, precipitation and local vegetation pattern data implies the effects of climate change and land cover on water resources. These parameters contribute to find more appropriate the accuracy of the equation 'quantity of rainfall' and 'quantity of water' which may infiltrate or may flow on surface as runoff. Reduction in groundwater recharge due to reduction of effective precipitation is the main effect which occurs from the increase of evapotranspiration in a designated area. More studies which investigated the climate change impact on water resources demonstrated decreases in the groundwater level, decrease of spring and rivers discharge. Reference evapotranspiration calculations at regional scale using GIS and remote sensing were computed by Zhan et al., (2015) for China land and by Ramírez-Cuesta et al., (2017) for South of Spain. Nistor et al., (2016) indicated increases of crop evapotranspiration (ET_c) in the Carpathian region due to climate changes along the last 50 years. In the Pannonian basin were also observed increases of ET_c between present and future (Nistor et al., 2017). /Studies related to evapotranspiration and water management in central Europe were carried out by Anda et al., (2015), Blanka et al., (2017).

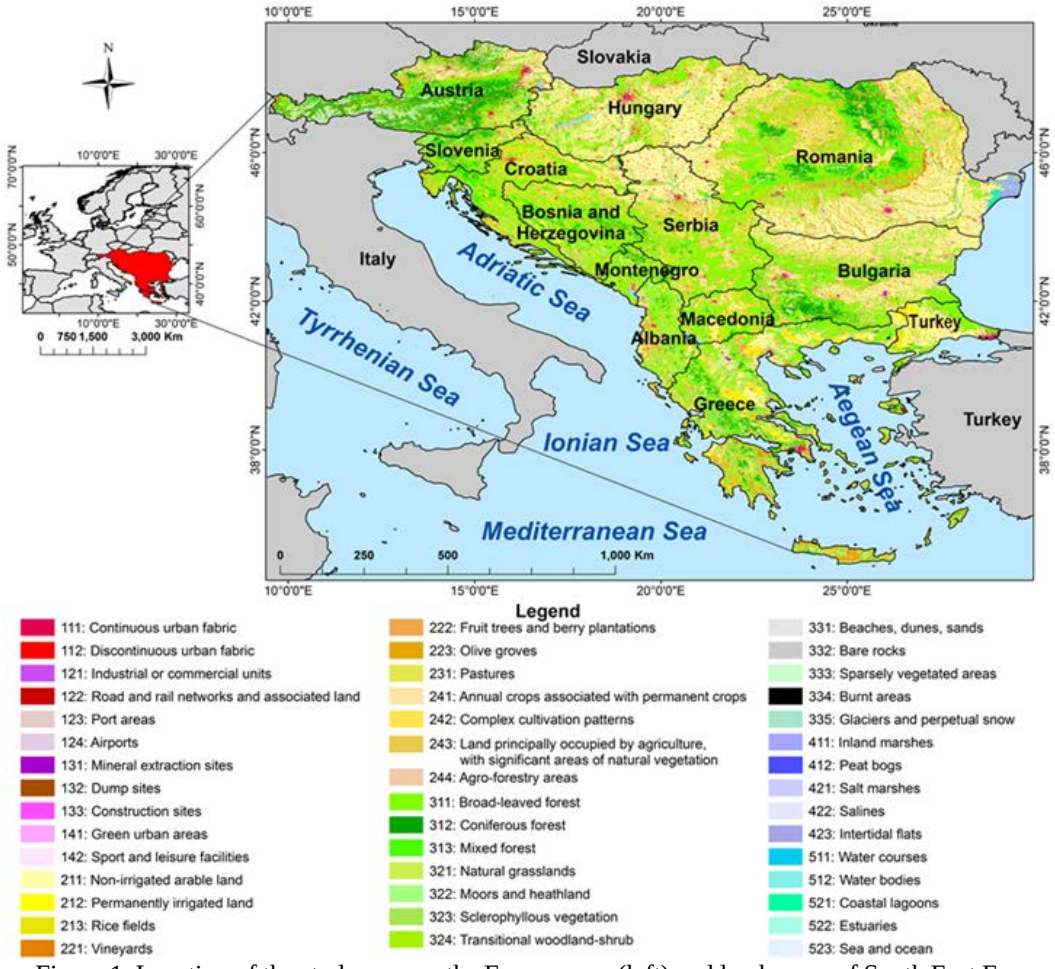

Figure 1. Location of the study area on the Europe map (left) and land cover of South East Europe region (right)

Based on the modelling of water table under climate change in Geer Basin from Belgium, it was observed that groundwater levels will decrease in the future period (Brouyère et al., 2004). In the Hungarian-Serbian cross-border area the drought severity influence on agricultural production have been analysed by Fiala et al., (2014). Based on Soil Water Balance European Water Accounting model, Kurnik et al., (2014) carried out the evapotranspiration of main agricultural regions from Europe. In Western Macedonia the evapotranspiration sensitive parameter was assessed by Ambas & Baltas (2012) using specifically methods. Recently, Güçlü et al., (2017) performed the evapotranspiration in Kingdom of Saudi Arabia using the regional fuzzy chain model. Ladányi et al., (2015) assessed the future drought hazard in the Kiskunság National Park and its surrounding landscapes from Hungary based on REMO and ALADIN regional climate model simulations.

The goal of the present paper was to integrating the climate models data of South East Europe and the European Land Cover dataset of vegetation representation into formula to calculate the climate change effects on ET_c. The applied methodology was tested in the Emilia-Romagna region by Nistor & Porumb-Ghiurco (2015) and further was successfully applied to other regions of Europe (Nistor et al., 2016, Nistor et al., 2017).

2. STUDY AREA

South East Europe region expands over West Black Sea and North Mediterranean Sea lands but includes also the countries from central and southcentral Europe. Čenčur Curk et al., (2014) in theirs report about climate change and groundwater in South East Europe delineated the region including also whole Austria.

The limits of the South East Europe region were set at 49°4' latitude N in North, at 34°52' latitude N in South, at 9°29' longitude E in West, and at 29°39' longitude E in East (Fig. 1). Over the study area there are the riverine countries belonging to the Mediterranean Sea basin (Slovenia, Croatia, Bosnia and Herzegovina, Montenegro, Albania, Greece), in central part of the region is located Serbia and Macedonia, in the eastern part is located Bulgaria and European part of Turkey and in the North of the region there are Austria, Hungary and Romania. Extending over 13 countries, the South East Europe region has a complex orography which includes the Eastern Alps in Austria and Slovenia, the Dinaric Mountains in Albania, Bosnia and Herzegovina, Croatia, Italy, Kosovo, Montenegro, Serbia and Slovenia, the Southern and Eastern Carpathians in Romania. Eastern Greece and mainly the Dalmatian and Aegean Islands are characterized by rocky aspects. The main lowlands in the study area extends in the central and South of Hungary, North of Serbia, East of Croatia, northeastern of Bosnia and Herzegovina, East and northeastern of Greece, South, West, and East of Romania, North and South of Bulgaria, and in European part of Turkey. In some few places of Macedonia and Albania there could be find limited plains. Hilly areas are also present in the region, especially located between mountains and plains.

South East Europe has a temperate climate with oceanic influence in West, with Baltic influence in North, and transnational influence in East, but the Mediterranean influence is the largest feel in the region. According to Kottek et al., (2006), the fully humid climate class with hot summers (Cfa) and fully humid climate class with warm summers (Cfb) climates extend over the Austria, Hungary, Serbia, Romania, Bulgaria, and Macedonia. In the South sides of South East Europe the main climate is Csa. Analysing the current period, the mean annual temperature in the study area ranged from -1.7 °C in northwest to 19°C in South. For the same period, the mean annual precipitation register the maximum values of 2324 mm $year^{-1}$ in the western sides of the region, near the Adriatic Sea, in the land of Slovenia and Croatia. The potential evapotranspiration (ET_0) in South East Europe ranged from 342 mm up to 1039 mm, showing the high values in the South of the region and in the low lands where the temperature are elevated during several months over the year. Figure 2 illustrates the annual averages of temperature, the annual averages of precipitation, and the annual averages of ET_0 registered in the South East Europe during the two analysed the periods (1991–2020 and 2021–2050).

The relief and climate of the region induce the typically vegetation growth in the respective area. Thus, in the elevated and in the mountains areas may be finding the coniferous and evergreen forests. The hilly areas are mainly covered by mixed and broad-leaved forests which included species as hornbeam (*Carpinus*), beech (*Fagus*), oak (*Quercus*), and elms (*Ulmus*) (European Environment Agency, 2007), but also is covered by pasture, shrubs, and transnational woodland. Typically for the lowlands and plains are agricultural crops, hay, and herbaceous vegetation. In the coastal areas there are located mainly the Mediterranean vegetation in West and South as Stone pine (Pinus pinea), green areas, and sclerophyllous vegetation. The coastal zones include also the harbours areas, the delta lagoons, marshes, beaches and dunes areas.

3. MATERIALS AND METHODS

3.1. Climate and land cover data

In the present study we used the mean annual temperature, mean annual precipitation, and mean ET_0 climate models related to two 30 years periods of 1991 to 2020 and 2021 to 2050. The spatial resolution of climate data is about 25 X 25 km and it were carried out by the National Meteorological Administration from Bucharest in the framework of the CC-WARE European project. The climate data models extend over the southeastern part of Europe (Čenčur Curk et al., 2014) and were projected based on the RegCM3, ALADIN, and PROMES models according to the A1B scenario proposed by IPCC, (2001). This scenario follows the population increase, economic growth, and adept technology up to mid of 21st century. The model of 1991 – 2020 period was used for the present and the model of 2021 – 2050 period for the future. The regional coupled models (RCMs) outputs were bias corrected using E-OBS data sets and the quintile mapping technique (Déqué, 2007; Formayer & Haas, 2010) based on daily observations (CCWaterS, 2010) and monthly temperature and precipitations derived from three RegCM3 models completed for the 1991 to 2050 period. Also, the very good RMSE values between observed and modelled data were verified. Gridded at 25 km spatial resolution, the three RCMs were computed by the National Center for Atmospheric Research during the late 1980s and early 1990s. This type of model is based on the dynamical downscaling, and it sustained by the Abdus Salam International Centre for Theoretical Physics (ICTP) from Trieste, Italy (Elguindi et al., 2007).

The ALADIN model was built at Centre National de Recherche Meteorologique (CNRM), and it served for the ARPEGE-Climate as a driver for the IPCC (2001) climate scenarios over the European domain (Spiridonov et al., 2005; Farda et al., 2010). The PROMES model is an atmospheric model processed by MOMAC (MOdelizacion para el Medio Ambiente y el Clima) research group from the Complutense University of Madrid (UCM) and the University of Castilla-La Mancha (UCLM) (Castro et al., 1993; Gaertner et al., 2010), and it is sustained by the GCM HADCM3Q0. The firsts combinations of the RegCM3, ADALDIN-Climate and PROMES were available from the ENSEMBLES project (Hewitt & Griggs, 2004), and they were chosen due to (i) their spatial extension of the South East Europe area, (ii) its performance in the representation and modelling of the historic climate conditions, and (iii) each one of these models are based on the GCM. The powerful of the RCMs models to reproduce the temperature and precipitation in various areas was tested with good results (Busuioc et al., 2010). The model-based values and seven meteorological stations in the study area are in line with the known uncertainties of the RCMs (Soares et al., 2012; Wilcke et al., 2013). The RMSE indicates values lower than 1°C for temperature, and around 100-150 mm for precipitation. The mountains areas represent the higher deviations of the RMSE.

In the identification of land type categories of South East Europe was used the Corine Land Cover 2012 of 4th level raster data with 250 m spatial resolution elaborated by Copernicus Land Monitoring Services. We agree with the Copernicus Land Monitoring Services because is easy to integrate in ArcGIS environment and it covers the large part of Europe.

The operations of ET_c were completed based on climate data models and Corine Land Cover with a 1 X 1 km spatial resolution. This set was adopted because for uniformity and accuracy in ET_c mapping, but also because this resolution was used for similar studies of ET_c in others European regions by Nistor, (2016) and Nistor et al., (2016).

3.2. Potential evapotranspiration data (ET_0)

In the calculation of seasonal and annual ET_c in South East Europe the ET_0 data grids of climate models were used. Based on Thornthwaite, (1948) formula (Eq. (1)) the monthly ET_0 related to present (1991-2020) and future (2021-2050) were find. This method is very useful in hydrology and climate (Čenčur Curk et al., 2014; Nistor et al., 2015). For the present study the raster's data of ET_0 were derived from temperature data carried out from the RegCM3, ALADIN, and PROMES models.

$$ET_0 = 16\left(\frac{L}{12}\right)\left(\frac{N}{30}\right)\left(\frac{10T_i}{I}\right)^{\alpha} \quad (1)$$

where:

ET_0	monthly potential evapotranspiration [mm]
L	average day length of the month being calculated [h]
N	number of days in the month being calculated
T_i	average monthly temperature [°C], ET_0=0 if $\bar{Tm}$ <0
I	heat index (Eq.(2))
α	complex function of heat index (Eq. (3))

$$I = \sum_{i=1}^{12}\left(\frac{T_i}{5}\right)^{1.514} \quad (2)$$

where:

T_i	monthly air temperature

$$\alpha = 6.75 \times 10^{-7} I^3 - 7.71 \times 10^{-5} I^2 + 1.7912 \times 10^{-2} I + 0.49239 \quad (3)$$

where:

I	annual heat index

3.3. Crop coefficient (K_c)

The key of ET_c calculation is coming from the reference values of evapotranspiration rate. Thus, in the specific literature (Allen et al., 1998) the vegetation or crop evapotranspiration rate is called the evapotranspiration or crop coefficient (K_c). In aim to calculate the ET_c, a value of K_c for each categories of land cover was assigned. Normally, the K_c is the result of the division between ET_c at ET_0 and may be extracted by tools in test sites in various conditions of dry and wet air. Because of this reason, the K_c takes more or less appropriate values, depending also about the annual period, latitude, and crop growth (Allen et al., 1998; Grimmond & Oke, 1999). To be in line with the specific literature, here we chosen the standard single K_c suggested by Allen et al., (1998) in the report of Food and Agriculture Organization. The reference rate from the urban areas and bare soil was studied in different places from the United States by Grimmond & Oke (1999), which published for the first the K_c values for urban areas and bare soil. Considering the appropriate latitude as a factor of relevance, the K_c values of the urban areas and bare soil were set according with Grimmond & Oke (1999). According with Nistor & Porumb-Ghiurco (2015) and Nistor et al., (2016), the spatial distribution of K_c and ET_c was mapping related to four seasons: initial, mid-season, end season, and cold season. The seasons were set following the crop growth during one year and considering the initial season from March to May, the mid-season from June to August, the end season from September to October and the cold season from November to February. In base of season's divisions, the values of initial season co-efficient ($K_{c\ ini}$), mid-season co-efficient ($K_{c\ mid}$), end season co-efficient ($K_{c\ end}$) and cold season co-efficient ($K_{c\ cold}$) were assigned to land cover of the South East Europe. Figure 3 indicates the spatial distribution of K_c in South East Europe region. Table 1 shows the values of K_c used in present study.

3.4. Crop evapotranspiration (ET_c)

ET_c is the result of the product between K_c and ET_0. The seasonal ET_c and annual ET_c were carried out using the Spatial Analyst Tools from ArcGIS environment. Because of the advantages in spatial data analysis and mapping, but also for mathematical operation, many papers call the powerful of this software (Baltas, 2007; Deniz et al., 2011, Dezsi et al., 2015; Nistor & Petcu, 2015). In order to find the seasonal ET_c, the initial ET_c ($ET_{c\ ini}$) (Eq. (4), the mid-season ET_c ($ET_{c\ mid}$) (Eq. (5), the end season ET_c ($ET_{c\ end}$) (Eq. (6), and the cold ET_c ($ET_{c\ cold}$) (Eq. (7) were calculated. Further, summing the four ET_c seasons for present and future were carried out the annual ET_c for both periods.

$$ET_{c\ ini} = ET_{0\ ini} \times K_{c\ ini} \quad (4)$$

$$ET_{c\ mid} = ET_{0\ mid} \times K_{c\ mid} \quad (5)$$

$$ET_{c\ end} = ET_{0\ end} \times K_{c\ end} \quad (6)$$

$$ET_{c\ cold} = ET_{0\ cold} \times K_{c\ cold} \quad (7)$$

$$Annual\ ET_c = ET_{c\ ini} + ET_{c\ mid} + ET_{c\ late} + ET_{c\ cold} \quad (8)$$

In aim to depict the locations with major changes between future and past annual ET_c, the absolute and relative changes were calculated. The absolute change map was calculated making the difference between future and present raster data of annual ET_c (Eq. (9). Successively, the relative changes was calculated divided the absolute change raster map at annual ET_c raster map related to present (Eq. (10).

$$ET_c\ absolute\ changes = future\ annual\ ET_c - present\ annual\ ET_c \quad (9)$$

$$ET_c\ relative\ changes = \frac{future\ annual\ ET_c - present\ annual\ ET_c}{present\ annual\ ET_c} \quad (10)$$

4. RESULTS AND DISCUSSION

Seasonal and annual ET_c results for present and future periods show how ET_c oscillate in response to climate change. For the future period, climate models indicate in several locations increases of mean annual temperature up to 0.9 °C and decreasing of mean annual precipitations by 50 mm. Due to increase of mean annual temperature the ET_0 increase by almost 100 mm in South East Europe region, fact for which the ET_c changes will expected between present and future.

Figure 4 depicts the spatial distribution of seasonal ET_c in South East Europe for both analysed periods. Going through the findings, in the present period (1991-2020), the $ET_{c\ ini}$ values ranges from 3 mm to 250 mm, while in the future period (2021-2050) the $ET_{c\ ini}$ ranges from 4 mm to 257 mm. In the mid-season the $ET_{c\ mid}$ ranges from 42 mm to 773 mm in the present period and $ET_{c\ mid}$ ranges from 45 mm to 857 mm in the future period.

The highest values of $ET_{c\ mid}$ (over 600 mm) in the present period are found in the southern sides of South East Europe, mainly in North and East sides of Greece, in South of Romania, eastern sides of Bulgaria and European Turkey, and in northeastern sides of Croatia. In the future period the high values of $ET_{c\ mid}$ could be found in North, East, and central parts of Greece, but also in the soutwestern parts of Romania. The $ET_{c\ end}$ ranges from 0 mm to 272 mm in the present period and ranges from 4 mm to 294 mm in the future period. As we expected, in the

future period the $ET_{c\ end}$ has higher values than in the present period.

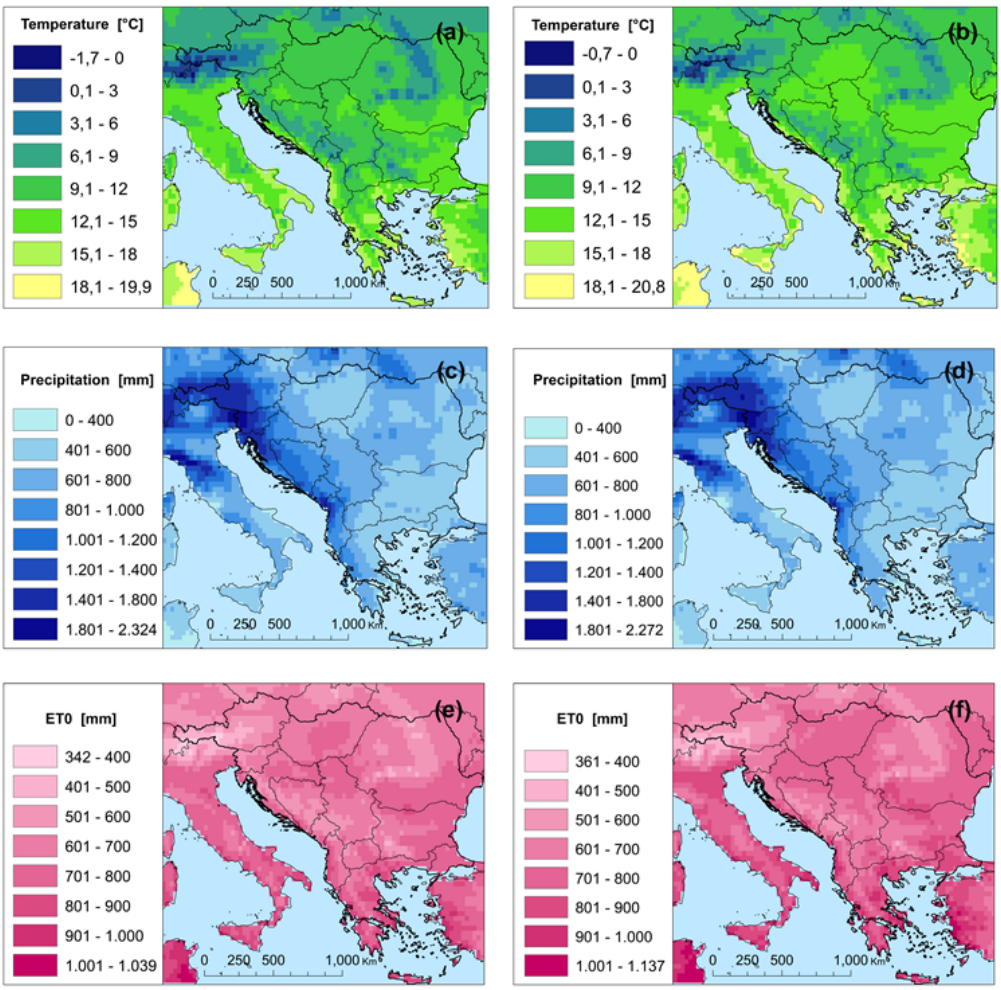

Figure 2. a. The average of mean annual air temperature between 1991-2020. b. The average of mean annual air temperature between 2021-2050. c. The average of mean annual precipitation between 1991-2020. d. The average of mean annual precipitation between 2021-2050. e. The average annual ET_0 between 1991-2020. f. The average annual ET_0 between 2021-2050.

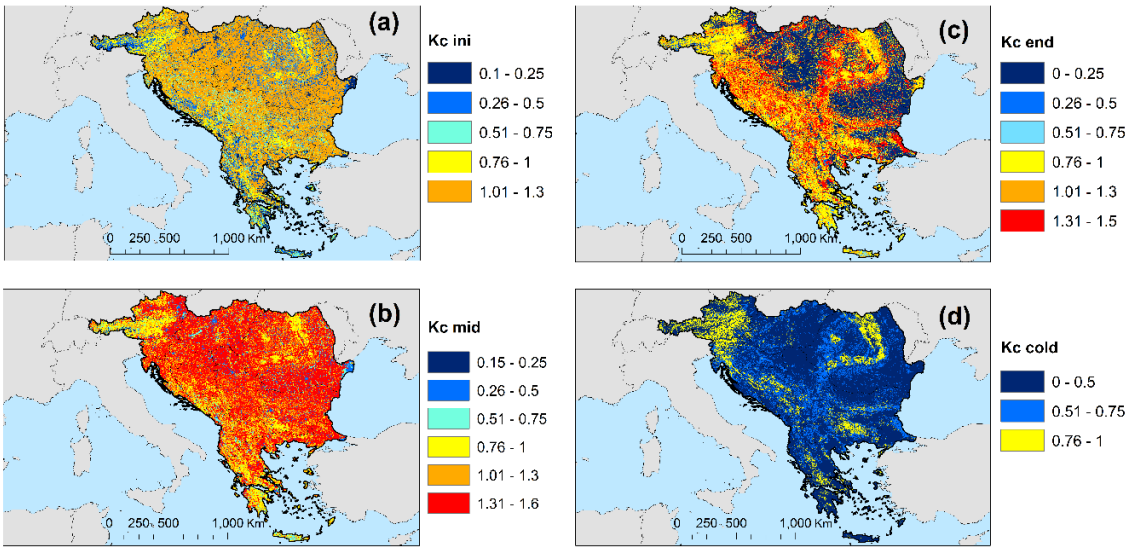

Figure 3. Spatial distribution of K_c in South East Europe. a. $K_{c\ ini}$ for the initial stage. b. $K_{c\ mid}$ for the mid-season stage. c. $K_{c\ end}$ for the late stage. d. $K_{c\ cold}$ for the cold stage.

Table 1. Corine Land Cover coefficients used for seasonal ETc in South East Europe.

Corine Land Cover		Kc ini season					Kc mid season					Kc end season					Kc cold season				
CLC code 2006	CLC Description	Kc	Ks	Ku	Kw	Kclc	Kc	Ks	Ku	Kw	Kclc	Kc	Ks	Ku	Kw	Kclc	Kc	Ks	Ku	Kw	Kclc
111	Continous urban fabric	-	-	0.2	-	0.2	-	-	0.4	-	0.4	-	-	0.25	-	0.25	-	-	-	-	-
112	Discontinuous urban fabric	-	-	0.1	-	0.1	-	-	0.3	-	0.3	-	-	0.2	-	0.2	-	-	-	-	-
121	Industrial or commercial units	-	-	0.2	-	0.2	-	-	0.4	-	0.4	-	-	0.3	-	0.3	-	-	-	-	-
122	Road and rail networks and associated land	-	-	0.15	-	0.15	-	-	0.35	-	0.35	-	-	0.25	-	0.25	-	-	-	-	-
123	Port areas	-	-	0.3	-	0.3	-	-	0.5	-	0.5	-	-	0.4	-	0.4	-	-	-	-	-
124	Airports	-	-	0.2	-	0.2	-	-	0.4	-	0.4	-	-	0.3	-	0.3	-	-	-	-	-
131	Mineral extraction sites	-	-	0.16	-	0.16	-	-	0.36	-	0.36	-	-	0.26	-	0.26	-	-	-	-	-
132	Dump sites	-	-	0.16	-	0.16	-	-	0.36	-	0.36	-	-	0.26	-	0.26	-	-	-	-	-
133	Construction sites	-	-	0.16	-	0.16	-	-	0.36	-	0.36	-	-	0.26	-	0.26	-	-	-	-	-
141	Green urban areas	-	-	0.12	-	0.12	-	-	0.32	-	0.32	-	-	0.22	-	0.22	-	-	-	-	-
142	Sport and leisure facilities	-	-	0.1	-	0.1	-	-	0.3	-	0.3	-	-	0.2	-	0.2	-	-	-	-	-
211	Non-irrigated arable land	1.1	-	-	-	1.1	1.35	-	-	-	1.35	0	-	-	-	0	-	-	-	-	-
212	Permanently irrigated land	1.2				1.2	1.45				1.45	1.35				1.35	-	-	-	-	-
213	Rice fields	1.05	-	-	-	1.05	1.2	-	-	-	1.2	0.6	-	-	-	0.6	-	-	-	-	-
221	Vineyards	0.3	-	-	-	0.3	0.7	-	-	-	0.7	0.45	-	-	-	0.45	-	-	-	-	-
222	Fruit trees and berry plantations	0.3	-	-	-	0.3	1.05	-	-	-	1.05	0.5	-	-	-	0.5	-	-	-	-	-
223	Olive groves	0.65	-	-	-	0.65	0.7	-	-	-	0.7	0.65	-	-	-	0.65	0.5	-	-	-	0.5
231	Pastures	0.4	-	-	-	0.4	0.9	-	-	-	0.9	0.8	-	-	-	0.8	-	-	-	-	-
241	Annual crops associated with permanent crops	0.5	-	-	-	0.5	0.8	-	-	-	0.8	0.7	-	-	-	0.7	-	-	-	-	-
242	Complex cultivation patterns	1.1	-	-	-	1.1	1.35	-	-	-	1.35	1.25	-	-	-	1.25	-	-	-	-	-
243	Land principally occupied by agriculture, with significant areas of natural vegetation	0.7	-	-	-	0.7	1.15	-	-	-	1.15	1	-	-	-	1	-	-	-	-	-
244	Agro-forestry areas	0.9	-	-	-	0.9	1.1	-	-	-	1.1	1.05	-	-	-	1.05	0.3	-	-	-	0.3
311	Broad-leaved forest	1.3	-	-	-	1.3	1.6	-	-	-	1.6	1.5	-	-	-	1.5	0.6	-	-	-	0.6
312	Coniferous forest	1	-	-	-	1	1	-	-	-	1	1	-	-	-	1	1	-	-	-	1
313	Mixed forest	1.2	-	-	-	1.2	1.5	-	-	-	1.5	1.3	-	-	-	1.3	0.8	-	-	-	0.8
321	Natural grasslands	0.3	-	-	-	0.3	1.15	-	-	-	1.15	1.1	-	-	-	1.1	-	-	-	-	-
322	Moors and heathland	0.8	-	-	-	0.8	1	-	-	-	1	0.95	-	-	-	0.95	-	-	-	-	-
323	Sclerophyllous vegetation	0.25	-	-	-	0.25	0.9	-	-	-	0.9	0.8	-	-	-	0.8	-	-	-	-	-
324	Transitional woodland-shrub	0.8	-	-	-	0.8	1	-	-	-	1	0.95	-	-	-	0.95	-	-	-	-	-
331	Beaches, dunes, sands	-	0.2	-	-	0.2	-	0.3	-	-	0.3	-	0.25	-	-	0.25	-	-	-	-	-
332	Bare rocks	-	0.15	-	-	0.15	-	0.2	-	-	0.2	-	0.05	-	-	0.05	-	-	-	-	-
333	Sparsely vegetated areas	0.4	-	-	-	0.4	0.6	-	-	-	0.6	0.5	-	-	-	0.5	-	-	-	-	-
334	Burnt area	-	0.1	-	-	0.1	-	0.15	-	-	0.15	-	0.05	-	-	0.05	-	-	-	-	-
335	Glaciers and perpetual snow	-	-	-	0.48	0.48	-	-	-	0.52	0.52	-	-	-	0.5	0.52	-	-	-	0.5	0.5
411	Inland marshes	-	-	-	0.15	0.15	-	-	-	0.45	0.45	-	-	-	0.8	0.8	-	-	-	-	-
412	Peat bogs	-	-	-	0.1	0.1	-	-	-	0.4	0.4	-	-	-	0.8	0.75	-	-	-	-	-
421	Salt marshes	-	-	-	0.1	0.1	-	-	-	0.3	0.3	-	-	-	0.7	0.7	-	-	-	-	-
422	Salines	-	0.1	-	-	0.1	-	0.15	-	-	0.15	-	0.05	-	-	0.05	-	-	-	-	-
423	Intertidal flats				0.3	0.3	-	-	-	0.7	0.7	-	-	-	1.3	1.3	-	-	-	-	-
511	Water courses	-	-	-	0.25	0.25	-	-	-	0.65	0.65	-	-	-	1.3	1.25	-	-	-	-	-
512	Water bodies	-	-	-	0.25	0.25	-	-	-	0.65	0.65	-	-	-	1.3	1.25	-	-	-	-	-
521	Coastal lagoons	-	-	-	0.3	0.3	-	-	-	0.7	0.7	-	-	-	1.3	1.3	-	-	-	-	-
522	Estuaries	-	-	-	0.25	0.25	-	-	-	0.65	0.65	-	-	-	1.3	1.25	-	-	-	-	-
523	Sea and ocean	-	-	-	0.4	0.4	-	-	-	0.8	0.8	-	-	-	1.4	1.4	-	-	-	-	-

Kc - crop coefficient for plants, Ks - evaporation coefficient for bare soils, Ku - crop coefficient for urban areas, Kw - evaporation coefficient for open water, Kclc - crop coefficient for land cover
Source: From Allen et al., (1998); Nistor & Porumb-Ghiurco (2015); Nistor et al., (2017).

Comparing the seasonal ET_0 and $K_{c\ end}$ patterns which can make the difference, is clearly that in the fall months (September and October) the ET_0 has insignificant increase in the future period. The lower values of $ET_{c\ end}$ fall below 30 mm in both periods. The minimum values of $ET_{c\ end}$ (0 mm) in the present period are located in the main plains of the South East Europe, including the South of Hungary, East of Austria, northeast of Croatia, North of Serbia, central Bulgaria, South and East sides of Romania and European part of Turkey, where the non-irrigated arable lands are found and where the main cereals (wheat, maize) and similar crops such fodder crops, root crops and fallow land are usually harvested after mid-season. High values of $ET_{c\ end}$ (over 150 mm) have been depicted especially in western part of the South East Europe (Slovenia, Croatia, Montenegro, Albania, Greece, South of Serbia, Central of Greece,), but also in the Carpathian Region. The spatial distribution of the high values of $ET_{c\ end}$ in the future period are much closed to the present, with few changes in the central and North of Greece.

Due to the lower temperature in the cold season, but also for the reduction of most types of vegetation functioning, the $ET_{c\ cold}$ in the present and the future register lower values. Interestingly, the values from 0 mm to 111 mm were identified for the $ET_{c\ cold}$ in the present and in the future. The high values of $ET_{c\ cold}$ were registered in the central and east sides of Greece, but also in the southeastern and eastern sides of Bulgaria respective European Turkey.

The annual ET_c values ranges from 56 mm to 1297 mm in the present period and ranges from 59 mm to 1410 mm in future period. The highest values of annual ET_c (over 1000 mm) for the present could be found in the central and northeastern of Greece, southwestern of Romania, East of Croatia, North of Bosnia and Herzegovina, West of Albania, southeast of Bulgaria, northeast of European Turkey, and east of Serbia. The spatial distribution of future annual ET_c shows more locations with high values. Thereby, in the South, West and southwest of Romania, eastern and northeastern sides of Greece, North and central sides of Bulgaria, East of Croatia, North of Bosnia and Herzegovina, East and West of European Turkey were identified values of ET_c higher than 1200 mm. The lower values of annual ET_c for the present and future are located in northwest of the region especially in the Alps Range, in North and central sides of the region especially in the Carpathian Mountains, but also in several mountain places from eastern part of the South East Europe and in the southwestern sides of Bulgaria. Figure 5 depicts the present and future annual ET_c distribution in South East Europe region.

The absolute and relative changes were carried out to check the areas with more impact under climate change between future and present periods. The areas with significant changes of absolute changes are located in South, southwestern and East sides of the South East Europe. Few absolute changes are founded in North and northeast sides of the South East Europe. The relative changes indicates that the central of Greece, but also the East of Albania registered changes with values higher than 0.08% between both future and present periods. Figure 6 shows the absolute and relative changes of annual ET_c between present and future periods.

Calculation of the seasonal and annual ET_c in South East Europe related to present and future periods was the main goal of the present study. Recent climate change indicated a warm of climate in many locations of the Globe, but also the future models shows rise in mean annual temperature up to 3°C and decrease in mean annual precipitation (IPCC, 2001; Stavig et al., 2005; IPCC, 2007; IPCC, 2014; The Canadian Centre for Climate Modelling and Analysis, 2014). The models created for the South East Europe indicates the maximum increase by 0.9°C of the mean annual temperature and a decrease by almost 50 mm of mean annual precipitation. These observations are in line with recent issues about climate (IPCC, 2001; IPCC, 2007; IPCC, 2014).

The seasonal ET_c mapping considering four stages of crop growth followed the methodology proposed by Nistor & Porumb-Ghiurco (2015), Nistor et al., (2016), and Nistor et al., (2017). In reality, the development stage of crops can be inserted between initial and mid-season, but because of overlapping in the growth crops calendar and because of heterogeneity of the land cover in South East Europe, it was agreed to include it in the initial season (Nistor & Porumb-Ghiurco, 2015; Nistor et al., 2016). Thus, insignificant variations between present and future in the $ET_{c\ ini}$ may be explained by climate changes in spring months (March to May) especially in mean monthly temperature which implies the changes in mean ET_0. Interestingly is that in the future period the values higher than 700 mm of $ET_{c\ mid}$ occupies more territories in comparison with the present period. Thus, the elevated $ET_{c\ mid}$ values are located in South, southwestern, and southeastern sides of Romania, North and East of Greece, West of European Turkey, east of Bulgaria, central of Serbia. The places with maximum values of $ET_{c\ mid}$ correspond to land covered by broad-leaved forest, complex cultivation patterns, and agro-forestry areas. The places with lower $ET_{c\ mid}$ are found in the Eastern Alps, Southern Carpathians and Dinaric Mountains, where are the elevated areas, lower temperatures and where the ET_0 fall below 400 mm $year^{-1}$.

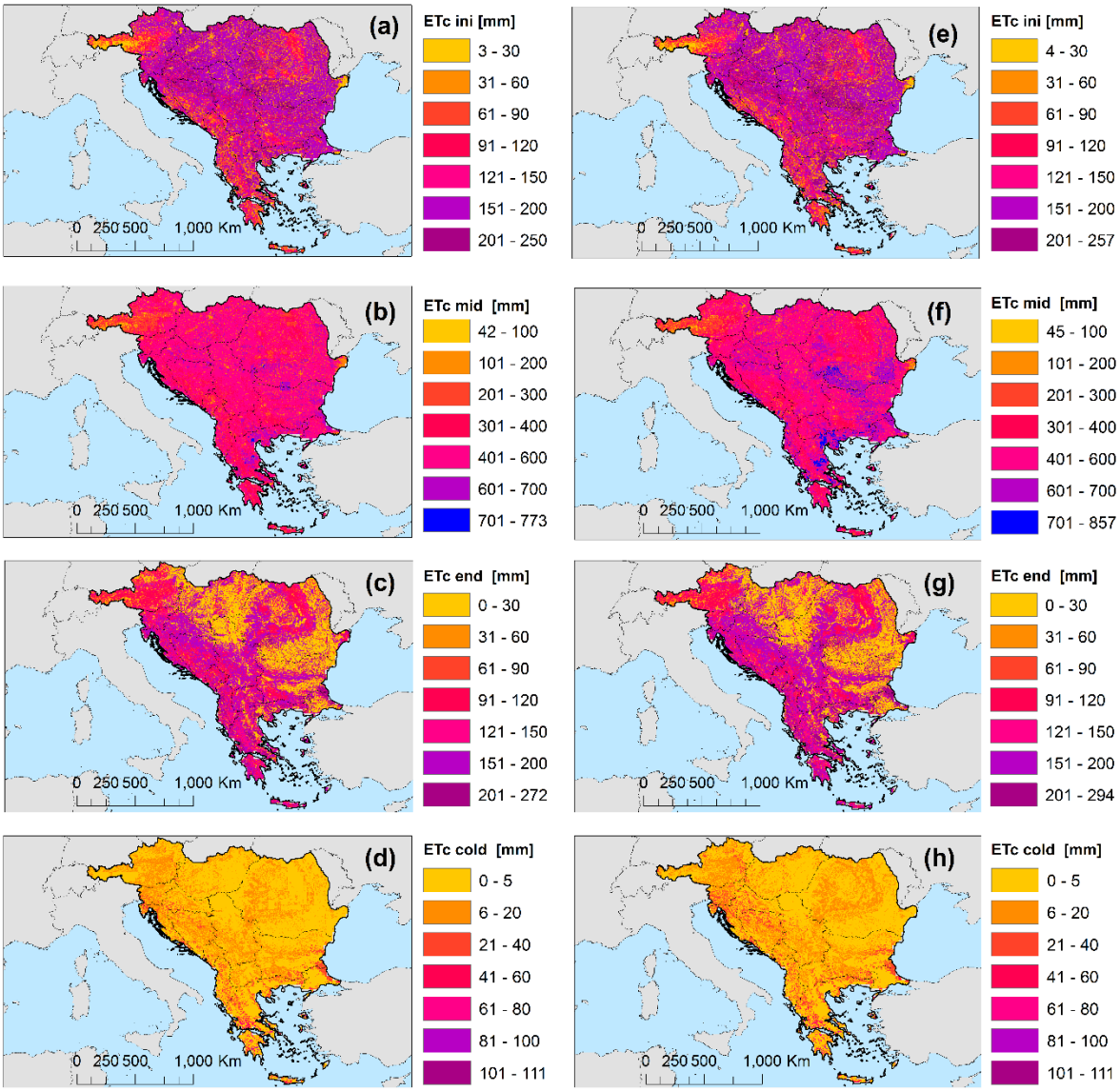

Figure 4. Spatial distribution of seasonal ETc in South East Europe. a. $ET_{c\ ini}$ for the initial stage (1991-2020). b. $ET_{c\ mid}$ for the mid-season stage (1991-2020). c. $ET_{c\ end}$ for the end stage (1991-2020). d. $ET_{c\ cold}$ for the cold stage (1991-2020). e. $ET_{c\ ini}$ for the initial stage (2021-2050). f. $ET_{c\ mid}$ for the mid-season stage (2021-2050). g. $ET_{c\ end}$ for the end stage (2021-2050). h. $ET_{c\ cold}$ for the cold stage (2021-2050).

Referring to the $ET_{c\ cold}$ spatial distribution, the highest values were located in the areas where the mean annual temperature is higher in cold season than in others areas, but also in that areas the K_c values are higher than in other areas due to presence of evergreen and broad-leaved forests which contributed to an increase of $ET_{c\ cold}$ even if the temperature are lower. The high values of annual ET_c (over 1200 mm) are identified in the South and South-East sides of the region, but also the values over 1200 mm of ET_c are found in central and West of South East Europe. The highest values of ET_c in respective areas are influenced by the high temperatures and high K_c of vegetation (e.g. broad-leaved forest). The annual and seasonal ET_c values obtained in the mountains ranges and for the lowlands in South East Europe are close to annual and seasonal ET_c values reported by Nistor et al., (2016), Nistor et al., (2017) for the Carpathian region and lowlands from Pannonian basin.

5. CONCLUSIONS

Based on the results, the recent and future climate influences negatively the ET_c in South East Europe. This impact of climate change has a strong imprint in the South and East sides of the region. In both periods, the $ET_{c\ mid}$ season indicates the heights values during the whole year, while in the $ET_{c\ cold}$ season the values are minimal.

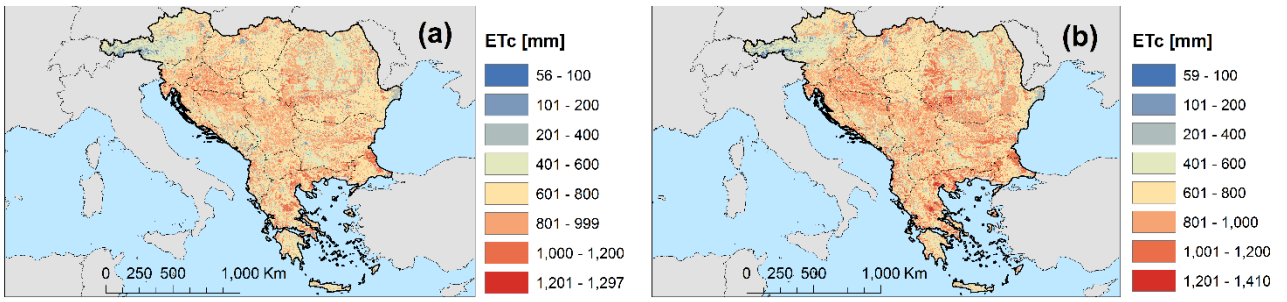

Figure 5. Spatial distribution of annual ET_c in South East Europe. a. Annual ET_c for the present period (1991-2020). b. Annual ET_c for the future period (2021-2050).

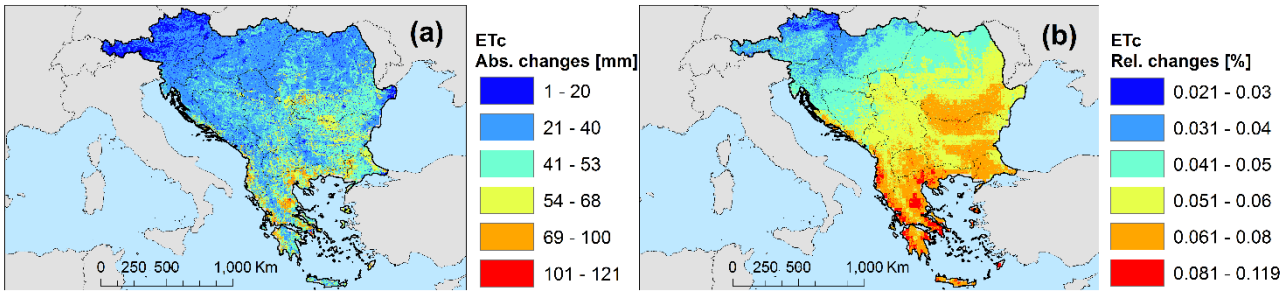

Figure 6. a. Absolute changes of annual ET_c in South East Europe between future and present period. b. Relative changes of annual ET_c in South East Europe between future and present period.

The gaps of the study may be assimilated in some aspects which regards the field research. Thus, due to large extension of the region, the field measurements with lysimeters of each land cover type were absent. Also, the evapotranspiration rate of water coming by irrigation was not considered by present research. These limitations do not affects the investigations because the standard K_c taking from literature were tested in many location of the world and together the empirical equations the methodology applied here gave good results at regional scale.

The main findings indicate values up to 1297 mm and 1410 mm for the annual ET_c in the present respective in the future periods, fact for which the agriculture lands, but also the areas with high intake of water should be in good managing for the following period. Considering the outcomes of this paper, the future investigations may be focused on the ET_c assessment of same crops in different countries in aim to mitigate and improve the new plans of strategy for South East Europe regarding agriculture and water resources. Moreover, the findings of the paper can be helpful for the climatologists, hydrogeologists, but also for the environmental scientists and policymakers which built the planning studies in one of the most important region of Europe.

Acknowledgements

The authors would like to thank to the European Environment Agency which provided the land cover data for the whole Europe. Previous affiliation of the corresponding author: Earth research Company, Department of Hydrogeology, Cluj-Napoca, Romania.

REFERENCES

Aguilera, H, & Murillo, J.M., 2009, *The effect of possible climate change on natural groundwater recharge based on a simple model: a study of four karstic aquifers in SE Spain.* Environmental Geology, 57(5), 963–974.

Allen, R.G., Pereira, L.S., Raes, D. & Smith, M., 1998, *Crop evapotranspiration: guidelines for computing crop water requirements*. FAO Irrigation and Drainage Paper 56, Rome, 300 p.

Ambas, V.Th. & Baltas, E., 2012, *Sensitivity analysis of different evapotranspiration methods using a new sensitivity coefficient.* Global NEST Journal, 14(3), 335–343.

Anda, A., Soos, G., Teixeira da Silva, J.A. & Kozma-Bognar, V., 2015, *Regional evapotranspiration from a wetland in Central Europe, in a 16-year period without human intervention*. Agricultural and Forest Meteorology, 205, 60–72.

Baltas, E., 2007, *Spatial distribution of climatic indices in the northern Greece*. Meteorological applications, 14, 69-78.

Blanka, V., Ladányi, Zs., Szilassi, P., Sipos, G., Rácz, A. & Szatmári, J., 2017, *Public Perception on Hydro-Climatic Extremes and Water Management Related to Environmental Exposure, SE Hungary*. Water Resources Management, 1–16.

Brouyère, S., Carabin, G. & Dassargues, A., 2004, *Climate change impacts on groundwater resources: modelled deficits in a chalky aquifer, Geer basin, Belgium.* Hydrogeology Journal, 12, 123–134.

Busuioc, A., Birsan, M.V., Carbunaru, D., Baciu, M. & Orzan, A., 2015, *Changes in the large scale thermodynamic instability and connection with rain shower frequency over Romania: verification of the Clausius–Clapeyron scaling*. Int. J. Climatol. doi: 10.1002/joc.4477.

Castro, M., Fernandez, C. & Gaertner, M.A., 1993, *Description of a mesoscale atmospheric numerical model.* In Diaz JI, Lions JL (eds) Mathematics, 1 climate and environment. Rech. Math. Appl. Ser., 27, 230–253.

CC-WaterS, 2010, *Climate change and impacts on water supply - Final report*. Lead Partner of CC-WaterS project Vienna, Waterworks, Austria. European Climate Adaption Platform, 357 p. URL: http://climate-adapt.eea.europa.eu/metadata/projects/climate-change-and-impacts-on-water-supply. Accessed 15 May 2016

Čenčur Curk, B., Cheval, S., Marjanović, P., Siegel, H., Gerhardt, E., Hochbichler, E. et al., 2014, *CC-WARE Mitigating Vulnerability of Water Resources under Climate Change, WP3 - Vulnerability of Water Resources in SEE, Report Version 5*. Published by South East Europe - Transnational Cooperation Programme. URL: http://www.ccware.eu/output-documentation/output-wp3.html.

Chen, S.B., Liu, Y.F. & Thomas, A., 2006, *Climatic change on the Tibetan plateau: potential evapotranspiration trends from 1961 to 2000*. Clim. Chang., 76, 291–319.

Collins, D.N., 2008, *Climatic warming, glacier recession and runoff from Alpine basins after the Little Ice Age maximum.* Annals of Glaciology, 48(1), 119–124.

Déqué, M., 2007, *Frequency of precipitation and temperature extremes over France in an anthropogenic scenario: Model results and statistical correction according to observed values*. Global Planet Change, 57, 16–26.

Deniz, A., Toros, H. & Incecik, S., 2011. *Spatial variations of climate indices in Turkey*. Int. J. Climatol., 31, 394–403.

Dezsi, Șt., Nistor, M.M., Man, T.C. & Rusu, R., 2015, *The GIS assessment of a winter sports resort location. Case study: Beliș District, Western Carpathians*. Carpathian Journal of Earth and Environmental Sciences, 10 (1), 223–230.

Dong, P., Wang, C. & Ding, J., 2013, *Estimating glacier volume loss used remotely sensed images, digital elevation data, and GIS modelling*. International Journal of Remote Sensing, 34(24), 8881–8892.

Elfarrak, H., Hakdaoui, M. & Fikri, A., 2014, *Development of Vulnerability through the DRASTIC Method and Geographic Information System (GIS) (Case Groundwater of Berrchid), Morocco*. Journal of Geographic Information System, 6, 45–58.

Elguindi, N., Bi, X., Giorgi, F., Nagarajan, B., Pal, J., Solmon, F., Rauscher, S. & Zakey, A., 2007, *RegCM Version 3.1 User's Guide.* Trieste: PWCG Abdus Salam ICTP, 57 p.

European Environment Agency, 2007, *The Pannonian region - the remains of the Pannonian Sea*. [Condé S, Richard D, Liamine N, Leclère AS, Sotolargo B, Pinborg U (eds)]. ZooBoTech HB Ed., Sweden, 18 p.

Farda, A., Déqué, M., Somot, S., Horányi, A., Spiridonov, V. & Tóth, H., 2010, *Model Aladin as Regional Climate Model for Central and Eastern Europe.* Stud. Geophys. AS CR, 313–332.

Fiala, K., Blanka, V., Ladányi, Z., Szilassi, S., Benyhe, B., Dolinaj, D. & Pálfai, I., 2014, *Drought Severity and its Effect on Agricultural Production in the Hungarian-Serbian Cross-Border Area*. Journal of Environmental Geography, 7(3-4), 43–51.

Formayer, H. & Haas, P., 2010, *Correction of RegCM3 model output data using a rank matching approach applied on various meteorological parameters.* In Deliverable D3.2 RCM output localization method (BOKU-contribution of the FP 6 CECILIA project on http://www.cecilia-eu.org/).

Gaertner, M.A., Dominguez, M. & Garvert, M., 2010, *A modelling case-study of soil moisture– atmosphere coupling*. Q. J. Roy. Meteor. Soc. 136(S1), 483–495. doi: 10.1002/qj.541.

Grimmond, CSB. & Oke, T.R., 1999, *Evapotranspiration rates in urban areas, impacts of urban growth on surface water and groundwater quality.* In Proceedings of IUGG 99 Symposium HS5, July 1999, Birmingham, England. IAHS Publications, 259, 235–243.

Güçlü, Y.S., Subyani, A.M. & Şen, Z., 2017, *Regional fuzzy chain model for evapotranspiration estimation*. Journal of Hydrology, 544, 233–241.

Haeberli, W.R., Frauenfelder, R., Hoelzle, M. & Maisch, M., 1999, *On rates and acceleration trends of global glacier mass changes.* Physical Geography, 81A, 585–595.

Hewitt, C.D. & Griggs, D.J., 2004, *Ensembles-Based Predictions of Climate Changes and Their Impacts (ENSEMBLES).* Max Planck Institute for Meteorology, Hamburg, 5 p.

Hidalgo, H.G., Das, T., Dettinger, M.D. et al., 2009, *Detection and attribution of streamflow timing changes to climate change in the western United States.* Journal of Climate, 22(13), 3838–3855.

IPCC., 2001, *Climate Change 2001: The Scientific Basis. Contribution of Working Group I to the Third Assessment Report of the Intergovernmental Panel on Climate Change* [Houghton JT, Ding Y, Griggs DJ et al (eds.)]. Cambridge University Press, Cambridge, United Kingdom and New York, NY, USA, 881 p.

IPCC., 2007, *Contribution of Working Group I to the Fourth Assessment Report of the IPCC*. In „Climate Change 2007: The Physical Science Basis" [Solomon S, Qin D, Manning M, Chen Z, Marquis M, Averyt KB, Tignor M, Miller HL (eds.)]. Cambridge University Press, Cambridge, United Kingdom and New York, NY, USA, 996 p.

IPCC., 2014, *Climate Change 2014: Impacts, Adaptation, and Vulnerability*. Contribution of Working Group II to the Fifth Assessment Report of the Intergovernmental Panel on Climate Change. Cambridge University Press, Cambridge, United Kingdom and New York, NY, USA, 1132 pp.

Jiménez Cisneros, B.E., Oki, T., Arnell, N.W. et al., 2014, *Freshwater resources*. In: Climate Change 2014: Impacts, Adaptation, and Vulnerability. Part A: Global and Sectoral Aspects. Contribution of Working Group II to the Fifth Assessment Report of the Intergovernmental Panel on Climate Change [Field, C.B., Barros, V.R., Dokken, D.J. et al. (eds.)]. Cambridge University Press, Cambridge, United Kingdom and New York, NY, USA, 229–269.

Kargel, J.S., Abrams, M.J., Bishop, M.P., Bush, A., Hamilton, G., Jiskoot, H., Kääb, A., Kieffer, H.H., Lee, E.M., Paul, F., Rau, F., Raup, B., Shroder, J.F., Soltesz, D., Stainforth, S., Stearns, L. & Wessels, R., 2005, *Multispectral imaging contributions to global*

land ice measurements from space. Remote Sensing of Environment, 99(1), 187–219.

Kløve, B., Ala-Aho, P., Bertrand, G., Gurdak, J.J., Kupfersberger, H., Kværner, J., Muotka, T., Mykrä, H., Preda, E., Rossi, P., Bertacchi Uvo, C., Velasco, E. & Pulido-Velazquez, M., 2014, *Climate change impacts on groundwater and dependent ecosystems*. Journal of Hydrology, 518, 250–266.

Kottek, M., Grieser, J., Beck, C., Rudolf, B. & Rubel, F., 2006, *World Map of the Köppen-Geiger climate classification updated*. Meteorol., Z., 15(3), 259–263.

Kurnik, B., Kajfež-Bogataj, L. & Horion, S., 2014, *An assessment of actual evapotranspiration and soil water deficit in agricultural regions in Europe*. Int. J. Climatol., doi: 10.1002/joc.4154.

Ladányi, Zs., Blanka, V., Meyer, B., Mezősi, G. & Rakonczai, J., 2015, *Multi-indicator sensitivity analysis of climate change effects on landscapes in the Kiskunság National Park, Hungary*. Ecological Indicators, 58, 8–20.

Nistor, M.M. & Porumb-Ghiurco, C.G., 2015, *How to compute the land cover evapotranspiration at regional scale? A spatial approach of Emilia-Romagna region*. GEOREVIEW Scientific Annals of Ştefan cel Mare University of Suceava Geography Series, 25(1), 38–54.

Nistor, M.M. & Petcu, I.M., 2015, *Quantitative analysis of glaciers changes from Passage Canal based on GIS and satellite images, South Alaska*. Applied Ecology and Environmental Research, 13(2), 535–549.

Nistor, M.M., Dezsi, Șt. & Cheval, S., 2015, *Vulnerability of groundwater under climate change* and land cover: a new spatial assessment method *applied on Beliş district (Western Carpathians, Romania).* Environmental Engineering and Management Journal, 14(12), 2959–2971.

Nistor, M.M., 2016, *Spatial distribution of climate indices in Emilia-Romagna region*. Meteorological applications, 23, 304–313.

Nistor, M.M., Gualtieri, A., Cheval, S., Dezsi, Șt. & Boţan, V.E., 2016, *Climate change effects on crop evapotranspiration in the Carpathian Region during 1961-2010*. Meteorological applications, 23, 462–469.

Nistor, M.M., Cheval, S., Gualtieri, A., Dumitrescu, A., Boţan, V.E., Berni, A., Hognogi, G., Irimuş, I.A. & Porumb-Ghiurco, C.G., 2017, *Crop evapotranspiration assessment under climate change in the Pannonian basin during 1991-2050*. Meteorological applications, 24(1), 84–91, doi: 10.1002/met.0008.

Oerlemans, J., 2005, *Extracting a Climate Signal from 169 Glacier Records*. Science, 308, 675–677.

Parmesan, C. & Yohe, G., 2003, *A globally coherent fingerprint of climate change impacts across natural systems.* Nature, 421(2), 37–42.

Păcurar, A., 2015, *The climate change and its impact on international dimension of tourism.* Carpathian Journal of Earth and Environmental Sciences, 10 (2), 281 - 292.

Piao, S., Ciais, P., Huang, Y. et al., 2010, *The impacts of climate change on water resources and agriculture in China*. Nature, 467(7311), 43–51.

Prăvălie, R., 2014, *Analysis of temperature, precipitation and potential evapotranspiration trends in southern Oltenia in the context of climate change*. Geographia Technica, 9(2), 68–84.

Prăvălie, R., Sîrodoev, I., Patriche, C. V., Bandoc, G. & Peptenatu D., 2014, *The analysis of the relationship between climatic water deficit and corn agricultural productivity in the Dobrogea Plateau*. Carpathian Journal of Earth and Environmental Sciences, 9 (4), 201–214.

Ramírez-Cuesta, J.M., Cruz-Blanco, M., Santos, C. & Lorite, I.J., 2017, *Assessing reference evapotranspiration at regional scale based on remote sensing, weather forecast and GIS tools*. International Journal of Applied Earth Observation and Geoinformation, 55, 32–42.

Shahgedanova, M., Stokes, C.R., Gurney, S.D. & Popovnin, V., 2005, *Interactions between mass balance, atmospheric circulation, and recent climate change on the Djankuat Glacier, Caucasus Mountains, Russia.* Journal of Geophysical Research, 110(D16107), 1–12.

Soares, P.M.M., Cardoso, R.M., Miranda, P.M.A., Viterbo, P. & Belo-Pereira, M., 2012, *Assessment of the ENSEMBLES regional climate models in the representation of precipitation variability and extremes over Portugal.* J. Geoph. Res. Atmosphere, 117(D7), doi: 10.1029/2011JD016768.

Spiridonov, V., Somot, S. & Déqué, M., 2005, *ALADIN-Climate: from the origins to present date*. ALADIN Newsletter no. 29.

Stavig, L., Collins, L., Hager, C., Herring, M., Brown, E. & Locklar, E., 2005, *The effects of climate change on Cordova, Alaska on the Prince William Sound*. Alaska Tsunami Papers, The National Ocean Sciences Bowl. https://seagrant.uaf.edu/nosb/papers/2005/cordova-nurds.html. Accessed 23 April 2014

The Canadian Centre for Climate Modelling and Analysis, 2014, *The First Generation Coupled Global Climate Model.* Published by Environment and Climate Change Canada. URL: http://www.ec.gc.ca/ccmac-cccma/default.asp?lang=En&n=540909E4-1. Accessed 20 March 2015

Thornthwaite, C.W., 1948, *An approach toward a rational classification of climate.* Geogr. Rev., 38, 55–94.

Wilcke, R.A.I., Mendlik, T. & Gobiet, A., 2013, *Multi-Variable Downscaling and Error-Correction of Regional Climate Models*. Clim. Change, 120(4), 871–887, doi: 10.1007/s10584-013-0845-x.

Xie, X., Li, Y.X., Li, R., Zhang, Y., Huo, Y., Bao, Y. & Shen, S., 2013, *Hyperspectral characteristics and growth monitoring of rice (Oryza sativa) under asymmetric warming*. International Journal of Remote Sensing, 34(23), 8449–8462.

Yustres, Á., Navarro, V., Asensio, L., Candel, M. & García, B., 2013, *Groundwater resources in the Upper Guadiana Basin (Spain): a regional modelling analysis.* Hydrogeology Journal, doi 10.1007/s10040-013-0987-y.

Zhan, C., Yin, J., Wang, F. & Dong, Q., 2015, *Regional estimation and validation of remotely sensed evapotranspiration in China*. Catena 133, 35–42.

Received at: 26. 01. 2017
Revised at: 03. 04. 2017

Accepted for publication at: 08. 04. 2017
Published online at: 13. 04. 2017